Title

Multifactorial Experimental Design to Optimize the Anti-Inflammatory and Proangiogenic Potential of Mesenchymal Stem Cell Spheroids

Journal

Stem Cells, 35(6)

ISSN

1066-5099

Authors

Murphy, Kaitlin C

Whitehead, Jacklyn

Falahee, Patrick C

et al.

Publication Date

2017-06-01

DOI

10.1002/stem.2606

Peer reviewed

HHS Public Access

Author manuscript

Stem Cells. Author manuscript; available in PMC 2018 June 01.

Published in final edited form as:

Stem Cells. 2017 June ; 35(6): 1493–1504. doi:10.1002/stem.2606.

Multifactorial Experimental Design to Optimize the Anti-Inflammatory and Proangiogenic Potential of Mesenchymal Stem Cell Spheroids

Kaitlin C. Murphy[1], **Jacklyn Whitehead**[1], **Patrick C. Falahee**[1], **Dejie Zhou**[1], **Scott I. Simon**[1], and **J. Kent Leach**[1,2,*]

[1]Department of Biomedical Engineering, University of California, Davis, Davis, CA 95616

[2]Department of Orthopaedic Surgery, School of Medicine, University of California, Davis Sacramento, CA 95817

Abstract

Mesenchymal stem cell therapies promote wound healing by manipulating the local environment to enhance the function of host cells. Aggregation of mesenchymal stem cells (MSCs) into three-dimensional spheroids increases cell survival and augments their anti-inflammatory and proangiogenic potential, yet there is no consensus on the preferred conditions for maximizing spheroid function in this application. The objective of this study was to optimize conditions for forming MSC spheroids that simultaneously enhance their anti-inflammatory and proangiogenic nature. We applied a Design of Experiments (DOE) approach to determine the interaction between three input variables (number of cells/spheroid, oxygen tension, and inflammatory stimulus) on MSC spheroids by quantifying secretion of prostaglandin E_2 (PGE_2) and vascular endothelial growth factor (VEGF), two potent molecules in the MSC secretome. DOE results revealed that MSC spheroids formed with 40,000 cells/spheroid in 1% oxygen with an inflammatory stimulus (Spheroid 1) would exhibit enhanced PGE_2 and VEGF production versus those formed with 10,000 cells/spheroid in 21% oxygen with no inflammatory stimulus (Spheroid 2). Compared to Spheroid 2, Spheroid 1 produced 5-fold more PGE_2 and 4-fold more VEGF, providing the opportunity to simultaneously upregulate the secretion of these factors from the same spheroid. The spheroids induced macrophage polarization, sprout formation with endothelial cells, and keratinocyte migration in a human skin equivalent model – demonstrating efficacy on three key cell types that are dysfunctional in chronic non-healing wounds. We conclude that DOE-based

Address for correspondence: J. Kent Leach, Ph.D., University of California, Davis, Department of Biomedical Engineering, 451 Health Sciences Drive, Davis, CA 95616, Phone: (530) 754-9149, Fax: (530) 754-5739, jkleach@ucdavis.edu.

Kaitlin C. Murphy: Conception and design, financial support, collection and/or assembly of data, data analysis and interpretation, manuscript writing

Jacklyn Whitehead: Collection and/or assembly of data

Patrick C. Falahee: Collection and/or assembly of data

Dejie Zhou: Collection and/or assembly of data

Scott I. Simon: Conception and design, financial support, data analysis and interpretation, manuscript writing, final approval of manuscript

J. Kent Leach: Conception and design, financial support, data analysis and interpretation, manuscript writing, final approval of manuscript

DISCLOSURE STATEMENT

The authors indicate no potential conflicts of interest.

analysis effectively identifies optimal culture conditions to enhance the anti-inflammatory and proangiogenic potential of MSC spheroids.

Graphical TOC

Multivariable analysis was used to determine culture conditions that optimize the anti-inflammatory and proangiogenic potential of mesenchymal stem cell spheroids for potential use in wound healing applications.

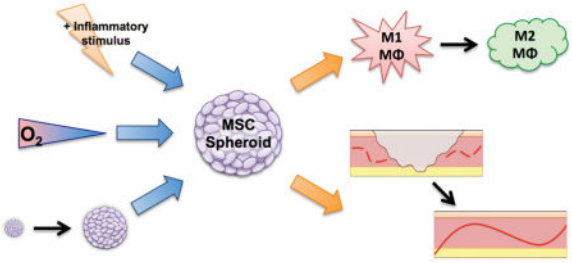

Keywords

mesenchymal stem cell; inflammation; proangiogenic; prostaglandin E_2; Design of Experiments

INTRODUCTION

Healing of a cutaneous wound is a well-orchestrated sequence of events involving coagulation, inflammation, migration and proliferation of multiple cell types, re-epithelialization, and remodeling.[1] Disruption of any step can lead to chronic non-healing wounds, occurring in 7 million patients each year in the United States.[2] Current non-surgical treatment options including aggressive debridement, adequate pressure offloading, antibiotics, hyperbaric oxygen therapy, and local wound dressings are effective in only 50% of patients, thereby motivating the need for alternative interventions.[3]

Chronic wounds have been treated using recombinant growth factors such as vascular endothelial growth factor (VEGF), platelet derived growth factor (PDGF), basic fibroblast growth factor (bFGF) and others, which enhanced neovascularization and epithelialization.[4] However, short half-lives and the need for supraphysiological concentrations represent substantial challenges for their clinical use.[5] As an alternative, stem cell therapy has shown promise in accelerating wound closure.[6] Mesenchymal stem cells (MSCs) can significantly enhance granulation tissue formation, angiogenesis, and reduce inflammation.[7–9] The therapeutic promise of MSCs is fulfilled through a diverse secretome containing numerous endogenous growth factors along with extracellular matrix (ECM) deposition to fill tissue defects.[5] However, the high death rate and poor engraftment of cells in ischemic conditions reduces the efficacy of stem cell therapy.[10] To increase transplanted cell survival and efficacy of stem cell therapy, we and others have demonstrated that MSCs exhibit increased overall function when formed into three dimensional (3D) spheroids.[11, 12] Beyond increased survival, spheroid formation also greatly enhances MSC secretion of bioactive factors for wound healing applications. Macrophage polarization, capillary formation, and re-

epithelialization are key steps in the wound healing cascade that are dysfunctional in chronic non-healing wounds. MSC spheroids produce up to 200-fold higher concentrations of anti-inflammatory proteins compared to dissociated MSCs including prostaglandin E_2 (PGE_2).[13, 14] PGE_2 is a potent anti-inflammatory mediator, stimulating native macrophages to shift from a pro-inflammatory M1 phenotype to an anti-inflammatory reparative M2 phenotype. The secretion of proangiogenic cues within the MSC secretome is also enhanced with spheroid formation, producing up to 100-fold more VEGF than dissociated cells *in vitro*[12] and enhancing vascularization *in vivo*.[15] Importantly, both PGE_2[16] and VEGF[17] promote re-epithelialization by stimulating keratinocyte migration and proliferation, further emphasizing the advantages of MSC spheroids for wound healing applications.

MSC spheroid function is dependent upon the culture microenvironment used to form these aggregates, the preferred combination of variables needed to generate spheroids for a specific application is unknown. We hypothesized that a combination of stimuli exists that promotes the overall anti-inflammatory and proangiogenic capacity of MSC spheroids. To test this hypothesis, we used a Design of Experiments (DOE) multivariable analysis approach to examine the significance and interaction of three input variables (spheroid size, oxygen microenvironment, and inflammatory stimulation to mimic the presence of local bacteria) on the anti-inflammatory and proangiogenic potential of MSC spheroids. These data demonstrate that DOE is an effective tool to optimize MSC spheroid wound healing potential, and that MSC spheroids can promote the function of multiple key resident cell types.

MATERIALS AND METHODS

Cell Culture

Human bone marrow-derived MSCs (Lonza, Walkersville, MD) were used without additional characterization. MSCs were expanded in α-MEM supplemented with 10% fetal bovine serum (FBS, Atlanta Biologicals, Flowery Branch, GA) and 1% penicillin/streptomycin (P/S, Gemini, Sacramento, CA) until use at passages 4–5. Endothelial colony forming cells (ECFCs), a subpopulation of endothelial progenitor cells, were generously provided by Dr. Mervin Yoder (Indiana University) and isolated using a protocol approved by the Institutional Review Board of the Indiana University School of Medicine and expanded until use at passages 12–13 as we reported.[18] Raw264.7 murine macrophages (ATCC, Manassas, VA) were used without further characterization and expanded as adherent cultures in Dulbecco's Modified Eagle Medium (DMEM) supplemented with 10% FBS and 1% P/S. Neonatal normal human epidermal keratinocytes (Lonza) were used without additional characterization. Keratinocytes were expanded in KBM-Gold basal medium with SingleQuot supplements (Lonza) until use at passage 6, and all keratinocyte differentiation mediums used DMEM (Thermo Fisher Scientific, Waltham, MA) as the basal medium. Human dermal fibroblasts (HDFs) were expanded in standard culture conditions in low glucose DMEM (Thermo Fisher Scientific) supplemented with 10% FBS, 1% P/S, and 1% 800 mM HEPES (Sigma Aldrich, St. Louis, MO) until use at passage 10.

Design of Experiments Model

A Box-Behnken experimental design was created with Design-Expert 8 software (Stat-Ease, Minneapolis, MN) to analyze the contribution of three continuous variables (number of cells per spheroid, oxygen microenvironment, and inflammatory stimulation) on the anti-inflammatory and proangiogenic potential of MSCs.[19] The three input variables were examined at low, medium, and high levels, with a centrally repeated condition to assess system variability. These variables were chosen due to their ability to modulate spheroid size, cell survival, and cytokine production in MSC spheroids.[12, 20, 21] The ranges for input variables were as follows: MSCs per spheroid from 10,000 to 40,000 (resulting in increasing spheroid diameter), oxygen tension from 1% to 21%, and addition of the inflammatory stimulus Pam_3-Cys-Ser-Lys_4 (Pam_3CSK_4), a Toll-like receptor 2 (TLR2) agonist used to mimic bacterial infection, at concentrations ranging from 0 to 1 μg/mL.[22] The resultant anti-inflammatory and proangiogenic potential of each condition was measured by quantifying PGE_2 and VEGF secretion, respectively. The significance and interaction of the three input variables on the measured output variables were determined *via* response surface predictions generated by the Design-Expert software.

Spheroid Formation

MSC spheroids were formed using the hanging drop technique with 10,000, 25,000, or 40,000 cells per 25 μL droplet.[12] During spheroid formation, cells were incubated in 1%, 11%, or 21% oxygen using oxygen-controlled HERAcell 150i incubators (Thermo Scientific, Pittsburgh, PA). The inflammatory stimulus Pam_3CSK_4 (Tocris, Minneapolis, MN) was added to the cell suspension prior to spheroid formation at a final concentration of 0, 0.5, or 1 μg/mL.

Characterization of MSC Spheroids

Cells were allowed to aggregate for 48 hours to allow for stabilization of spheroid diameter.[23] Conditioned media (CM) was collected and centrifuged at 10,000*g* for 10 minutes. Upon removal of the supernatant, spheroids were lysed with 200 μL passive lysis buffer (Promega, Madison, WI). DNA content was determined using the Quant-iT PicoGreen DNA Assay Kit (Invitrogen) and apoptosis was quantitatively measured from the same lysate using a Caspase-Glo 3/7 assay (Promega). In order to measure cellular metabolic activity, spheroids were collected and placed in 12-well plates with 1 mL of α-MEM containing AlamarBlue (10% v/v, Invitrogen); fluorescence was detected on a microplate reader and normalized to total DNA content from the same sample. Cell viability was assessed by a Live-Dead assay (Invitrogen). Spheroids were imaged using a Nikon Eclipse TE2000U microscope (Melville, NY) and Andor Zyla digital camera (Oxford Instruments, Abingdon, Oxfordshire, United Kingdom), and spheroid diameter was calculated in NIS Elements (Nikon).

Culture media was collected after spheroid formation, and the concentrations of PGE_2 and VEGF in the media were determined using protein-specific ELISA kits per the manufacturer's instructions (R&D Systems, Minneapolis, MN). Quantification of anti-inflammatory proteins within conditioned media was performed using a Human Cytokine Antibody Array (RayBiotech, Norcross, GA).[24] Pooled conditioned media from 4 replicates

was applied to one array well. Protein quantification was performed with a GenePix 4000B scanner and associated GenePix Pro software (Molecular Devices, Sunnyvale, CA) to calculate median minus background fluorescent intensity at 532 nm for each cytokine. Data were normalized to positive controls and exclude protein concentrations found in serum contained in unconditioned α-MEM.

Macrophage Inflammatory Assay

Raw264.7 murine macrophages were suspended in DMEM and stimulated with 100 ng/mL lipopolysaccharide (LPS, Invitrogen). After 10 minutes, the stimulus was removed *via* centrifugation at 250*g* for 5 minutes and unstimulated or stimulated macrophages were plated at 25,000 cells/cm^2 in 12-well culture plates. CM from Spheroid 1 and Spheroid 2 was collected and diluted in α-MEM such that the ratio of growth factor-producing cells to CM volume was kept constant. The CM was then added to stimulated macrophages at a 1:10 dilution. After 24 hours of culture, the macrophage CM was collected and assessed for pro- and anti-inflammatory markers. PGE_2 (1 ng/mL, Sigma) was used as a positive control. The polarization of the macrophages was determined by measuring pro-inflammatory TNFα and anti-inflammatory IL-10 using mouse protein-specific ELISA kits (R&D Systems).

Endothelial Cell Functional Assays

We evaluated the proangiogenic potential of MSC spheroids using a tubule formation assay as described.[25] Briefly, 100 μL of Growth Factor Reduced Matrigel (BD Biosciences) was pipetted into 48-well plates and allowed to gel at 37°C for 1 hour. ECFCs were seeded on Matrigel at 30,000 cells/cm^2 in GF-Def EGM-2, and a mixture of CM and GF-Def EGM-2 was added in a 1:4 volume ratio. Cells were cultured for 16 hours, after which they were stained with calcein AM (3 μg/mL in PBS; Invitrogen) for 30 minutes. Average number of branch points per field of view and average tubule length were quantified using NIS Elements (Nikon). EGM-2 served as the positive control, GF-Def EGM-2 served as an assay control, and EBM-2 served as a negative control.

Three-dimensional Human Skin Equivalent Model (HSE)

We fabricated modified human skin equivalents (HSEs) based on previously published protocols[26, 27] to evaluate the capacity of MSC spheroids to promote re-epithelialization in a 3D skin-like environment. HSEs were fabricated in six well plate inserts (Corning Incorporated, Corning, NY). Acellular collagen gels were formed with 1 mL of 3 mg/mL collagen (Advanced Biomatrix, Carlsbad, CA) per insert. Human dermal fibroblasts (HDF, passage 10, 94,000 cells) were suspended in 3 mL of 3 mg/mL collagen in each insert. Neonatal human epidermal keratinocytes (passage 6) were seeded on top of the layered acellular and cellular collagen gels at 350,000 cells per insert, and HSE constructs were maintained with keratinocyte differentiation medium for 14 days and at the air-liquid interface for the last 7 days.[26] Each HSE construct was wounded with an 8 mm biopsy punch (Integra Miltex, Plainsboro, New Jersey). MSC spheroids and dissociated cells (5×10^6 cells/mL) were suspended in 100 μL collagen (3 mg/mL), allowed to gel in 8 mm molds for 1 hour at 37°C, and then placed into the wounded HSE. Wound healing continued for 14 days at the air-liquid interface. HSE constructs were then placed in 10% buffered formalin (Fisher Scientific, Hampton, NH) for 24 hours while still in the six well plate inserts,

bisected along the greatest width of the wound, and processed for paraffin embedding and hematoxylin and eosin (H&E) staining. The extent of wound closure was quantified on digitized photographs of the H&E stained HSE taken on a Nikon Eclipse TE2000-U microscope with a Zyla Image Source color camera and processed using NIH ImageJ and Adobe Photoshop software. Measurement of wound length covered by the newly formed epidermis was quantified with a digital caliper as the distance between wound margins and expressed as a fraction of the initial 8 mm wound margin. Keratinocyte migration was confirmed by immunohistochemistry using an antibody to cytokeratin 10 (ab9026; 10 μg/mL; Abcam, Cambridge, UK).

Interrogating Pathways for PGE_2 and VEGF Upregulation by MSC Spheroids

To further explore the mechanism contributing to increased PGE_2 and VEGF secretion, we interrogated two critical pathways: NFκB and TNFκ. MSC spheroids were formed with 40,000 cells/spheroid and cultured under hypoxia in the presence of potent mediators (all from Tocris except TNFα (Abcam)) of the two pathways (Table 1). After spheroid formation, the spheroids and media were collected, and we quantified Caspase 3/7 activity, PGE_2, and VEGF secretion as described above. Additionally, TNFα concentrations were determined from the same sample using a human TNFα ELISA kit per the manufacturer's protocol (R&D Systems).

Statistical Analysis

Data are presented as mean ± standard deviation of the mean. Statistical analysis was performed using a one-way ANOVA with either a Tukey correction for multiple comparisons, a two-way ANOVA with Bonferonni correction for multiple comparisons, or paired t-tests when appropriate. All statistical analysis was performed in Prism 7 software (GraphPad); p values less than 0.05 were considered statistically significant. Significance is denoted by alphabetical letterings; groups with no significance are linked by the same letters, while groups with significance do not share the same letters.

RESULTS

Prediction of Spheroid Function by Experimental Design

A DOE-approach was used to determine the significance and interaction of spheroid size (achieved through manipulation of cell number per spheroid), oxygen microenvironment, and inflammatory stimulation on the wound healing potential of MSC spheroids. A Box-Behnken experimental design generated 13 unique culture conditions for spheroid formation with a centrally repeated condition, and the anti-inflammatory and proangiogenic potential was measured by quantifying PGE_2 and VEGF secretion, respectively.

Manipulating cell culture conditions resulted in spheroids that secreted a range of PGE_2 from 908 to 5973 pg (a 6.6-fold difference). Both number of cells per spheroid and concentration of the inflammatory stimulus Pam_3CSK_4 had a significant positive linear relationship with PGE_2 secretion, while oxygen tension had no significant effect (Fig. 1A). VEGF secretion ranged from 134 to 691 pg (a 5.2-fold difference). The number of cells per spheroid had a positive linear effect on VEGF secretion, while oxygen tension had a

negative linear relationship. The concentration of the inflammatory stimulus Pam_3CSK_4, which binds and activates Toll-like receptor 2 (TLR2), had no significant effect (Fig. 1C). Overall, the Model F-values of 4.43 and 8.02 suggest the models are significant for PGE_2 and VEGF secretion, respectively, and there is only a 2.58% and 0.34% chance that a Model F-Value this large could occur due to noise. The fits of the models were visualized by plotting predicted versus actual values upon quantifying PGE_2 and VEGF secretion *via* ELISA (Fig. 1B, D).

Secretory Potential Increases with Increasing Spheroid Size

To determine whether the predicted positive relationship between number of cells per spheroid and PGE_2 and VEGF secretion was due to culture geometry or the presence of more MSCs, total cell number was fixed at 200,000 cells/sample (Fig. 2A). The number of cells per spheroid was varied from 10,000 to 40,000 cells/spheroid, and spheroids were formed in 1% oxygen either with or without 1 μg/mL Pam_3CSK_4. DNA content was negatively affected by the addition of Pam_3CSK_4, and overall DNA content was statistically similar between groups of different spheroid sizes with the exception of the larger spheroid formed without Pam_3CSK_4 (Fig. 2B). PGE_2 secretion increased with increasing spheroid size, and the presence of Pam_3CSK_4 increased PGE_2 levels in the medium-sized spheroid (Fig. 2C). When normalized to DNA content, PGE_2 secretion also increased with increasing spheroid size, and Pam_3CSK_4 had a significant effect in spheroids formed with 10,000 and 25,000 cells/spheroid (Fig. 2D). VEGF secretion exhibited a similarly positive correlation for spheroids formed with Pam_3CSK_4. However, when spheroids were formed without the inflammatory stimulus, we detected greater amounts of VEGF in spheroids formed with 25,000 cells than the smaller or larger spheroids (Fig. 2E). This phenomenon was no longer apparent when normalized to DNA content, as spheroids formed with or without Pam_3CSK_4 exhibited increasing normalized VEGF secretion as the number of cells/spheroid increased (Fig. 2F).

Validation of DOE Model Results

Spheroids were formed from conditions predicted by the DOE to be the best- (Spheroid 1) and worst-performing (Spheroid 2) in terms of total PGE_2 and VEGF secretion. Spheroid 1 was formed with 40,000 cells/spheroid, 1 μg/mL Pam_3CSK_4, under 1% oxygen; Spheroid 2 was formed with 10,000 cell/spheroid, no inflammatory stimulus, under 21% oxygen. Total cell number was fixed at 200,000 cells/sample. Spheroid 1 produced 4-fold more VEGF (Fig. 3A) and 5-fold more PGE_2 (Fig. 3B) than Spheroid 2. Taken together with Fig. 2, these data validate our DOE model and demonstrate that by altering three key input variables, MSC spheroids can be induced to increase many-fold secretion of PGE_2 and VEGF. We further characterized the secretome of these MSC spheroids. A stacked column chart reveals that Spheroid 1 produced notably more anti-inflammatory cytokines; particularly IFN-γ and GRO (Fig. 3C). Additionally, we noted that spheroid formation generally upregulated the production of anti-inflammatory molecules compared to adherent monolayers formed under the same conditions (Supplementary Fig. S1). Subsequent experiments were performed using only Spheroid 1 and Spheroid 2.

Viability of Spheroid 1 and Spheroid 2

We quantified metabolic activity, caspase 3/7 activity as an indicator of apoptosis, and DNA content to determine if cell viability was affected by increases in spheroid size. The spheroids exhibited comparable metabolic and caspase 3/7 activity, and DNA content was comparable since the total number of cells was fixed at 200,000 cells/sample (Supplementary Fig. S2). In agreement with our quantitative biochemical assays, we observed no discernable differences in cell viability using live/dead dyes (Fig. 3D–E). Spheroid diameter decreased with decreasing cell number, ranging from 600 μm for Spheroid 1 down to 300 μm for Spheroid 2 (Fig. 3F).

MSC Spheroids Stimulate Polarization of Activated Macrophages

Conditioned media (CM) from Spheroid 1 reduced the expression of TNFα in LPS-stimulated murine macrophages to levels comparable to the positive control (Fig. 4A). CM from Spheroid 2 was unable to significantly reduce the expression compared to the stimulated control group. CM from adherent monolayers treated identically to their spheroid counterparts was also unable to reduce TNFα expression, demonstrating the importance of culture geometry. As expected, macrophages stimulated with LPS increased their expression of the pro-inflammatory marker TNFα nearly 7-fold, and the addition of 1 ng/mL PGE_2 returned TNFα levels to those of resident unstimulated macrophages.

CM from Spheroid 1 also upregulated IL-10 expression, an anti-inflammatory marker, while media from Spheroid 2 was unable to achieve the same anti-inflammatory response (Fig. 4B). CM from adherent monolayers treated as their spheroid counterparts failed to increase IL-10 expression. The unstimulated and stimulated macrophages secreted similar levels of IL-10, yet treatment with 1 ng/mL PGE_2 increased IL-10 secretion in stimulated macrophages. Taken together, CM from Spheroid 1 decreased TNFα expression and increased IL-10 expression from stimulated macrophages, indicating that the macrophages were polarized from the pro-inflammatory M1 phenotype to the anti-inflammatory M2 phenotype.

MSC Spheroids Increase Tubule Formation by Endothelial Colony Forming Cells

We characterized the functional bioactivity of secreted proangiogenic growth factors by testing the ability of CM to stimulate tubule formation by endothelial colony forming cells (ECFCs). We observed increases in the number of branch points when ECFCs were treated with CM from Spheroid 1 compared to Spheroid 2. Additionally, there were no statistical differences between cells treated with CM from Spheroid 1 and the positive control, EGM-2 (Fig. 5A). ECFCs stimulated with CM from Spheroid 1 formed significantly longer tubes compared to those stimulated with CM from Spheroid 2 and our positive control, EGM-2 (Fig. 5B). CM from adherent monolayers treated as their spheroid counterparts induced fewer branch points and tubule length compared to either spheroid or the positive control yet outperformed the negative control (EBM-2). ECFCs in EBM-2 did not exhibit any tubule formation, confirming that the cytokines in the conditioned medium were inducing network formation, not the Matrigel itself. These trends are qualitatively illustrated in Fig. 5C–E. Thus, the CM from Spheroid 1 was significantly more proangiogenic than that from

Spheroid 2, and spheroids were more proangiogenic than the traditional adherent monolayers.

MSC Spheroids Enhance Wound Healing in a Human Skin Equivalent Model

After 2 weeks in culture, defects treated with Spheroid 1 exhibited a significantly smaller wound diameter and increased wound closure, whereas healing in defects treated with dissociated MSCs preconditioned under the same conditions was not statistically different from untreated HSEs (Fig. 6A–D). Furthermore, collagen gels containing dissociated MSCs contracted to less than 2 mm in diameter over 14 days, resulting in a significant portion of the wound area being uncovered (*data not shown*). Immunostaining of HSE sections with cytokeratin 10, a marker of differentiated keratinocytes, revealed no keratinocytes at the defect margins in untreated HSEs, yet positive staining was detected at the base of the wound, suggesting that keratinocytes migrated from the wound edge to the air-liquid interface (Fig. 6E). We observed the most intense staining at the wound margins for defects treated with MSC spheroids (Fig. 6G), while significantly less positive staining was discernible in defects treated with dissociated MSCs (Fig. 6F). Taken together, these data indicate that the optimized Spheroid 1 could promote re-epithelialization in an *in vitro* model of wound healing.

MSC Spheroid PGE_2 Secretion is Mediated by NFκB signaling

PGE_2 secretion by Spheroid 1 was upregulated by stimulating the TNFα or NFκB pathways using known agonists (Fig. 7A). VEGF secretion was increased by stimulating with TNFα, yet neither VEGF nor TNFα secretion was mediated by stimulating the NFκB pathway (Fig. 7B, C). MSC spheroids treated with Pam_3CSK_4 exhibited a similar response to those treated with betulinic acid (BA), a known agonist of the NFκB pathway.

DISCUSSION

MSCs have tremendous potential for use in cell-based therapies for wound healing and tissue regeneration, largely due to the potent secretome available to surrounding cells when transplanted to the defect site. MSC spheroids exhibit improved survival and trophic factor secretion compared to dissociated cells, yet the appropriate combination of factors required to optimize secretion of trophic factors by MSC spheroids is unknown. In this study, we determined a combination of microenvironmental stimuli that increases the *in vitro* anti-inflammatory and proangiogenic potential of MSC spheroids by assessing the quantity and bioactivity of VEGF and PGE_2, two key factors within the MSC secretome that exhibit potent effects on cells within the wound environment. By tuning three independent input variables, we significantly enhanced the wound healing potential of MSC spheroids established by measuring the quantity and bioactivity of specific elements within the secretome.

PGE_2 secretion was selected due to its potency in modulating the function of multiple resident cell types during wound resolution.[28] MSC spheroids exhibit increased expression of PGE_2 compared to adherent monolayers or dissociated cells,[12, 13] making it an ideal target when optimizing spheroidal culture conditions for wound healing applications.

Increasing the number of MSCs per spheroid from 10,000 to 25,000 enhanced their anti-inflammatory potential as measured by TNFα-stimulated gene protein 6 (TSG-6) expression, yet spheroids composed of more than 100,000 cells exhibited markedly reduced TSG-6 levels.[13] Furthermore, the culture geometry of the MSC spheroids induces COX2 production, a critical enzyme in the generation of both PGE_2 and TSG6.[29] Thus, we chose the number of cells per spheroid as a key input variable, since we previously reported that increasing the number of MSCs per spheroid altered spheroid diameter.[12] While others reported that PGE_2 secretion in MSC spheroids is dependent on the activity of caspases,[14] we did not observe this phenomenon when comparing Spheroid 1 and Spheroid 2. However, we previously observed increases in caspase activity when changing a single input variable, number of cells per spheroid.[12] The oxygen tension under which the spheroids were formed had no significant effect on PGE_2 production, implying that it is the locally induced oxygen gradient that is responsible for this stress, not the overall availability of oxygen.

PGE_2 secretion was further modulated by the addition of Pam_3CSK_4, a synthetic bacterial lipopeptide and TLR2 agonist.[30] Pam_3CSK_4 functions similarly to the TLR-4 agonist lipopolysaccharide (LPS), in that it increases MSC production of hematopoietic growth factors such as granulocyte-colony stimulating factor (G-CSF) and Interleukin-11 (IL-11), whose pathways are typically activated by the innate immune response to gram-positive bacteria such as *S. aureus*.[31, 32] Others have preconditioned MSC spheroids with the pro-inflammatory cytokines IFN-γ and TNFα to increase PGE_2 production.[33] To our knowledge, this is the first work to show the positive effect of Pam_3CSK_4 on MSC spheroids, which targets a more specific cellular mechanism of inflammatory response.[32] We sought to explore if the underlying mechanism could be explained through the crossover in the TLR2 and TNFα-mediated PGE_2 production, as they both depend on TNF-related apoptosis-inducing ligand (TRAIL)[13, 31] and NFκB.[34] We found that while Pam_3CSK_4 acts in concert with the underlying NFκB pathway, the resulting upregulation of PGE_2 was not mediated by TNFα production. Both PGE_2 and TNFα expression were upregulated in Spheroid 1, but the presence of Pam_3CSK_4 alone did not upregulate TNFα production. Furthermore, spheroids treated with Pam_3CSK_4 exhibited a similar response to those treated with betulinic acid, an agonist of the NFκB pathway.[35] While others have reported that Pam_3CSK_4 increases MSC proliferation,[34] we noted a significant decrease in DNA content when MSC spheroids were formed in the presence of Pam_3CSK_4. This may be because spheroid formation decreases cell proliferation, likely through contact inhibition.[13] Interestingly, treatment with Pam_3CSK_4 had little to no effect on the DNA content in the largest 40,000-cell spheroid, suggesting that the mechanism by which Pam_3CSK_4 is activating the NFκB pathway is overridden when the cells in the spheroid are under greater oxidative stress. Additionally, our DOE did not predict the interaction between spheroid size and inflammatory stimulus, implying that the interaction between the two input variables was not statistically significant on the model as a whole.

VEGF secretion was chosen as the second output variable in our DOE model due to its potency in mediating blood vessel and capillary formation within the wound bed.[8, 36] The formation of capillary networks is a critical step in the wound healing process that is often disrupted in chronic non-healing wounds.[37] Similar to PGE_2, spheroid formation upregulates VEGF production compared to dissociated cells,[11, 12] and MSCs increase VEGF expression

in response to cellular stress.[38] MSCs stimulated with TNFα or hypoxia produce VEGF through an NFκB dependent mechanism.[39] In these studies, VEGF production increased as we increased spheroid size. Thus, we examined if the upregulation of VEGF was due to autocrine TNFα signaling by supplementing the media with C87, a lead chemical compound that directly binds to TNFα and effectively blocks all TNFα-triggered signaling pathways.[40] While supplemental TNFα enhanced VEGF production, the addition of C87 had no significant effect on VEGF production, suggesting that autocrine TNFα signaling was not responsible for increased VEGF production in optimized MSC spheroids. Therefore, the increased VEGF secretion in larger spheroids cultured under 1% oxygen is most likely due to the established HIF-1α pathway.

We used PGE_2 and VEGF as our two key outputs for the DOE approach, yet MSCs secrete a host of growth factors and cytokines that regulate multiple cell types involved in wound closure.[1] For example, we observed an upregulation of numerous cytokines affecting macrophages (IL-1α, IL-1β, IL-10, IFN-γ, MIP-1α), T-cells (IL-1α, IL-1β, IL-2), neutrophils (MIP-1α, IL-8, GRO), monocytes (MIP-1α), endothelial cells (TNFα, IL-8), and keratinocytes (VEGF, PGE_2, KGF).[1] Macrophages, endothelial cells, and keratinocytes are key cell types that are dysfunctional in chronic non-healing wounds frequently observed in decubitus ulcers of diabetic patients.[41, 42] The overall bioactivity of our optimized MSC spheroids was probed by culturing these cells in the presence of CM from Spheroid 1 or Spheroid 2. Upon demonstrating the potency of endogenous paracrine factors from MSC spheroids on macrophages and endothelial cells, we further characterized their potential as a cell based therapy for wound healing by investigating Spheroid 1's ability to promote re-epithelialization in a 3-dimensional skin equivalent model. Macrophages are involved in tightly regulating all phases of wound healing and can polarize towards a pro-inflammatory M1 phenotype or an anti-inflammatory M2 phenotype in response to cytoactive cues.[43] Macrophage dysfunction is partly responsible for chronic non-healing wounds; thus, overall wound healing and reduced fibrosis may be improved by enhancing macrophage polarization. Here we demonstrate that by engineering the MSC spheroid microenvironment, we can enhance MSC regulation of stimulated macrophages. Although MSC secretion of PGE_2 has been directly attributed to their anti-inflammatory properties, they secrete a multitude of other anti-inflammatory molecules that could further enhance their immunomodulatory properties.[44] In addition to being depleted of M1 macrophages, chronic non-healing wounds are also depleted of proangiogenic growth factors and thus have impaired revascularization. Similar to their anti-inflammatory properties, MSCs secrete many growth factors besides VEGF[45] that stimulate resident endothelial cells to form capillary networks and bring in essential oxygen and nutrients to the wound bed.[7] Lastly, MSC spheroids' vast secretome is also beneficial to keratinocytes, leading to the promotion of re-epithelialization.[46]

Conclusion

Using a multivariable DOE approach, we identified a combination of culture parameters that enables manipulation of the secretory function of MSC spheroids. Specifically, MSC spheroids were formed to simultaneously enhance secretion of proangiogenic and anti-inflammatory cues while optimizing their viability. Furthermore, engineered spheroids

enhanced the function of macrophages and endothelial cells, while hastening the healing of a wounded *in vitro* skin equivalent model. Therefore, strategies that simultaneously promote the anti-inflammatory and proangiogenic potential of MSC spheroids may enhance their clinical translation.

Supplementary Material

Refer to Web version on PubMed Central for supplementary material.

Acknowledgments

Research Support: This work was supported by NIH Grant R01-DE025475 (JKL) and R01-AI047294 (SIS). KM was supported by the American Heart Association Western States Affiliate Predoctoral Fellowship (15PRE21920010). JW was supported by a National Science Foundation Graduate Research Fellowship (1650042). The content is solely the responsibility of the authors and does not necessarily represent the official views of the National Institutes of Health. The funders had no role in the decision to publish, or preparation of the manuscript.

This work was supported by the National Institutes of Health under award numbers R01 DE025475 (JKL) and R01 AI047294 (SIS). The content is solely the responsibility of the authors and does not necessarily represent the official views of the National Institutes of Health. The funders had no role in the decision to publish, or preparation of the manuscript. KM was supported by the American Heart Association Western States Affiliate Predoctoral Fellowship (15PRE21920010). JW was supported by a National Science Foundation Graduate Research Fellowship (1650042).

References

1. Maxson S, Lopez EA, Yoo D, et al. Concise review: role of mesenchymal stem cells in wound repair. Stem Cells Transl Med. 2012; 1:142–149. [PubMed: 23197761]
2. Malhotra S, Bello E, Kominsky S. Diabetic foot ulcerations: biomechanics, charcot foot, and total contact cast. Semin Vasc Surg. 2012; 25:66–69. [PubMed: 22817854]
3. Apelqvist J. Diagnostics and treatment of the diabetic foot. Endocrine. 2012; 41:384–397. [PubMed: 22367583]
4. Moura LI, Dias AM, Carvalho E, et al. Recent advances on the development of wound dressings for diabetic foot ulcer treatment--a review. Acta Biomater. 2013; 9:7093–7114. [PubMed: 23542233]
5. Caplan AI, Dennis JE. Mesenchymal stem cells as trophic mediators. J Cell Biochem. 2006; 98:1076–1084. [PubMed: 16619257]
6. Chen L, Tredget EE, Wu PY, et al. Paracrine factors of mesenchymal stem cells recruit macrophages and endothelial lineage cells and enhance wound healing. PLoS One. 2008; 3:e1886. [PubMed: 18382669]
7. Wu Y, Chen L, Scott PG, et al. Mesenchymal stem cells enhance wound healing through differentiation and angiogenesis. Stem Cells. 2007; 25:2648–2659. [PubMed: 17615264]
8. Kwon DS, Gao X, Liu YB, et al. Treatment with bone marrow-derived stromal cells accelerates wound healing in diabetic rats. Int Wound J. 2008; 5:453–463. [PubMed: 18593394]
9. Amos PJ, Kapur SK, Stapor PC, et al. Human adipose-derived stromal cells accelerate diabetic wound healing: impact of cell formulation and delivery. Tissue Eng Part A. 2010; 16:1595–1606. [PubMed: 20038211]
10. Potier E, Ferreira E, Meunier A, et al. Prolonged hypoxia concomitant with serum deprivation induces massive human mesenchymal stem cell death. Tissue Eng. 2007; 13:1325–1331. [PubMed: 17518749]
11. Ho SS, Murphy KC, Binder BY, et al. Increased survival and function of mesenchymal stem cell spheroids entrapped in instructive alginate hydrogels. Stem Cells Transl Med. 2016; 5:773–781. [PubMed: 27057004]
12. Murphy KC, Fang SY, Leach JK. Human mesenchymal stem cell spheroids in fibrin hydrogels exhibit improved cell survival and potential for bone healing. Cell Tissue Res. 2014; 357:91–99. [PubMed: 24781147]

13. Bartosh TJ, Ylostalo JH, Mohammadipoor A, et al. Aggregation of human mesenchymal stromal cells (MSCs) into 3D spheroids enhances their antiinflammatory properties. Proc Natl Acad Sci U S A. 2010; 107:13724–13729. [PubMed: 20643923]
14. Ylostalo JH, Bartosh TJ, Coble K, et al. Human mesenchymal stem/stromal cells cultured as spheroids are self-activated to produce prostaglandin E2 that directs stimulated macrophages into an anti-inflammatory phenotype. Stem Cells. 2012; 30:2283–2296. [PubMed: 22865689]
15. Bhang SH, Lee S, Shin JY, et al. Transplantation of cord blood mesenchymal stem cells as spheroids enhances vascularization. Tissue Eng Part A. 2012; 18:2138–2147. [PubMed: 22559333]
16. Santos JM, Camoes SP, Filipe E, et al. Three-dimensional spheroid cell culture of umbilical cord tissue-derived mesenchymal stromal cells leads to enhanced paracrine induction of wound healing. Stem Cell Res Ther. 2015; 6:90. [PubMed: 25956381]
17. Michaels JT, Dobryansky M, Galiano RD, et al. Topical vascular endothelial growth factor reverses delayed wound healing secondary to angiogenesis inhibitor administration. Wound Repair Regen. 2005; 13:506–512. [PubMed: 16176459]
18. Decaris ML, Lee CI, Yoder MC, et al. Influence of the oxygen microenvironment on the proangiogenic potential of human endothelial colony forming cells. Angiogenesis. 2009; 12:303–311. [PubMed: 19544080]
19. Decaris ML, Leach JK. Design of experiments approach to engineer cell-secreted matrices for directing osteogenic differentiation. Ann Biomed Eng. 2011; 39:1174–1185. [PubMed: 21120695]
20. Baraniak PR, McDevitt TC. Scaffold-free culture of mesenchymal stem cell spheroids in suspension preserves multilineage potential. Cell Tissue Res. 2012; 347:701–711. [PubMed: 21833761]
21. Tsai AC, Liu Y, Yuan X, et al. Compaction, fusion, and functional activation of three-dimensional human mesenchymal stem cell aggregate. Tissue Eng Part A. 2015; 21:1705–1719. [PubMed: 25661745]
22. Kim MH, Granick JL, Kwok C, et al. Neutrophil survival and c-kit(+)-progenitor proliferation in Staphylococcus aureus-infected skin wounds promote resolution. Blood. 2011; 117:3343–3352. [PubMed: 21278352]
23. Vorwald CE, Ho SS, Whitehead JR, et al. High throughput formation of mesenchymal stem cell spheroids and entrapment in alginate hydrogels. Methods in Molecular Biology. 2017 In Press.
24. Jose S, Hughbanks ML, Binder BY, et al. Enhanced trophic factor secretion by mesenchymal stem/stromal cells with Glycine-Histidine-Lysine (GHK)-modified alginate hydrogels. Acta Biomater. 2014; 10:1955–1964. [PubMed: 24468583]
25. Murphy KC, Stilhano RS, Mitra D, et al. Hydrogel biophysical properties instruct coculture-mediated osteogenic potential. FASEB J. 2016; 30:477–486. [PubMed: 26443826]
26. Carlson MW, Alt-Holland A, Egles C, et al. Three-dimensional tissue models of normal and diseased skin. Curr Protoc Cell Biol. 2008; Chapter 19(Unit 19):19.
27. Maione AG, Brudno Y, Stojadinovic O, et al. Three-dimensional human tissue models that incorporate diabetic foot ulcer-derived fibroblasts mimic in vivo features of chronic wounds. Tissue Eng Part C Methods. 2015; 21:499–508. [PubMed: 25343343]
28. Syeda MM, Jing X, Mirza RH, et al. Prostaglandin transporter modulates wound healing in diabetes by regulating prostaglandin-induced angiogenesis. Am J Pathol. 2012; 181:334–346. [PubMed: 22609345]
29. Bartosh TJ, Ylostalo JH, Bazhanov N, et al. Dynamic compaction of human mesenchymal stem/precursor cells into spheres self-activates caspase-dependent IL1 signaling to enhance secretion of modulators of inflammation and immunity (PGE2, TSG6, and STC1). Stem Cells. 2013; 31:2443–2456. [PubMed: 23922312]
30. Nguyen DT, de Witte L, Ludlow M, et al. The synthetic bacterial lipopeptide Pam3CSK4 modulates respiratory syncytial virus infection independent of TLR activation. PLoS Pathog. 2010; 6:e1001049. [PubMed: 20808895]
31. Wang X, Cheng Q, Li L, et al. Toll-like receptors 2 and 4 mediate the capacity of mesenchymal stromal cells to support the proliferation and differentiation of CD34(+) cells. Exp Cell Res. 2012; 318:196–206. [PubMed: 22100911]

32. Romieu-Mourez R, Francois M, Boivin MN, et al. Cytokine modulation of TLR expression and activation in mesenchymal stromal cells leads to a proinflammatory phenotype. J Immunol. 2009; 182:7963–7973. [PubMed: 19494321]
33. Zimmermann JA, McDevitt TC. Pre-conditioning mesenchymal stromal cell spheroids for immunomodulatory paracrine factor secretion. Cytotherapy. 2014; 16:331–345. [PubMed: 24219905]
34. Pevsner-Fischer M, Morad V, Cohen-Sfady M, et al. Toll-like receptors and their ligands control mesenchymal stem cell functions. Blood. 2007; 109:1422–1432. [PubMed: 17038530]
35. Wan Y, Wu YL, Lian LH, et al. The anti-fibrotic effect of betulinic acid is mediated through the inhibition of NF-kappaB nuclear protein translocation. Chem Biol Interact. 2012; 195:215–223. [PubMed: 22285267]
36. Barrientos S, Brem H, Stojadinovic O, et al. Clinical application of growth factors and cytokines in wound healing. Wound Repair Regen. 2014; 22:569–578. [PubMed: 24942811]
37. Bauer SM, Bauer RJ, Velazquez OC. Angiogenesis, vasculogenesis, and induction of healing in chronic wounds. Vasc Endovascular Surg. 2005; 39:293–306. [PubMed: 16079938]
38. Binder BY, Genetos DC, Leach JK. Lysophosphatidic acid protects human mesenchymal stromal cells from differentiation-dependent vulnerability to apoptosis. Tissue Eng Part A. 2014; 20:1156–1164. [PubMed: 24131310]
39. Crisostomo PR, Wang Y, Markel TA, et al. Human mesenchymal stem cells stimulated by TNF-alpha, LPS, or hypoxia produce growth factors by an NF kappa B- but not JNK-dependent mechanism. Am J Physiol Cell Physiol. 2008; 294:C675–682. [PubMed: 18234850]
40. Ma L, Gong H, Zhu H, et al. A novel small-molecule tumor necrosis factor alpha inhibitor attenuates inflammation in a hepatitis mouse model. J Biol Chem. 2014; 289:12457–12466. [PubMed: 24634219]
41. Raja, Sivamani K, Garcia MS, et al. Wound re-epithelialization: modulating keratinocyte migration in wound healing. Front Biosci. 2007; 12:2849–2868. [PubMed: 17485264]
42. Patel S, Maheshwari A, Chandra A. Biomarkers for wound healing and their evaluation. J Wound Care. 2016; 25:46–55. [PubMed: 26762498]
43. Lucas T, Waisman A, Ranjan R, et al. Differential roles of macrophages in diverse phases of skin repair. J Immunol. 2010; 184:3964–3977. [PubMed: 20176743]
44. Prockop DJ, Oh JY. Mesenchymal stem/stromal cells (MSCs): role as guardians of inflammation. Mol Ther. 2012; 20:14–20.
45. Hoch AI, Binder BY, Genetos DC, et al. Differentiation-dependent secretion of proangiogenic factors by mesenchymal stem cells. PLoS One. 2012; 7:e35579. [PubMed: 22536411]
46. Chen D, Hao H, Fu X, et al. Insight into reepithelialization: how do mesenchymal stem cells perform? Stem Cells Int. 2016; 2016:6120173. [PubMed: 26770209]

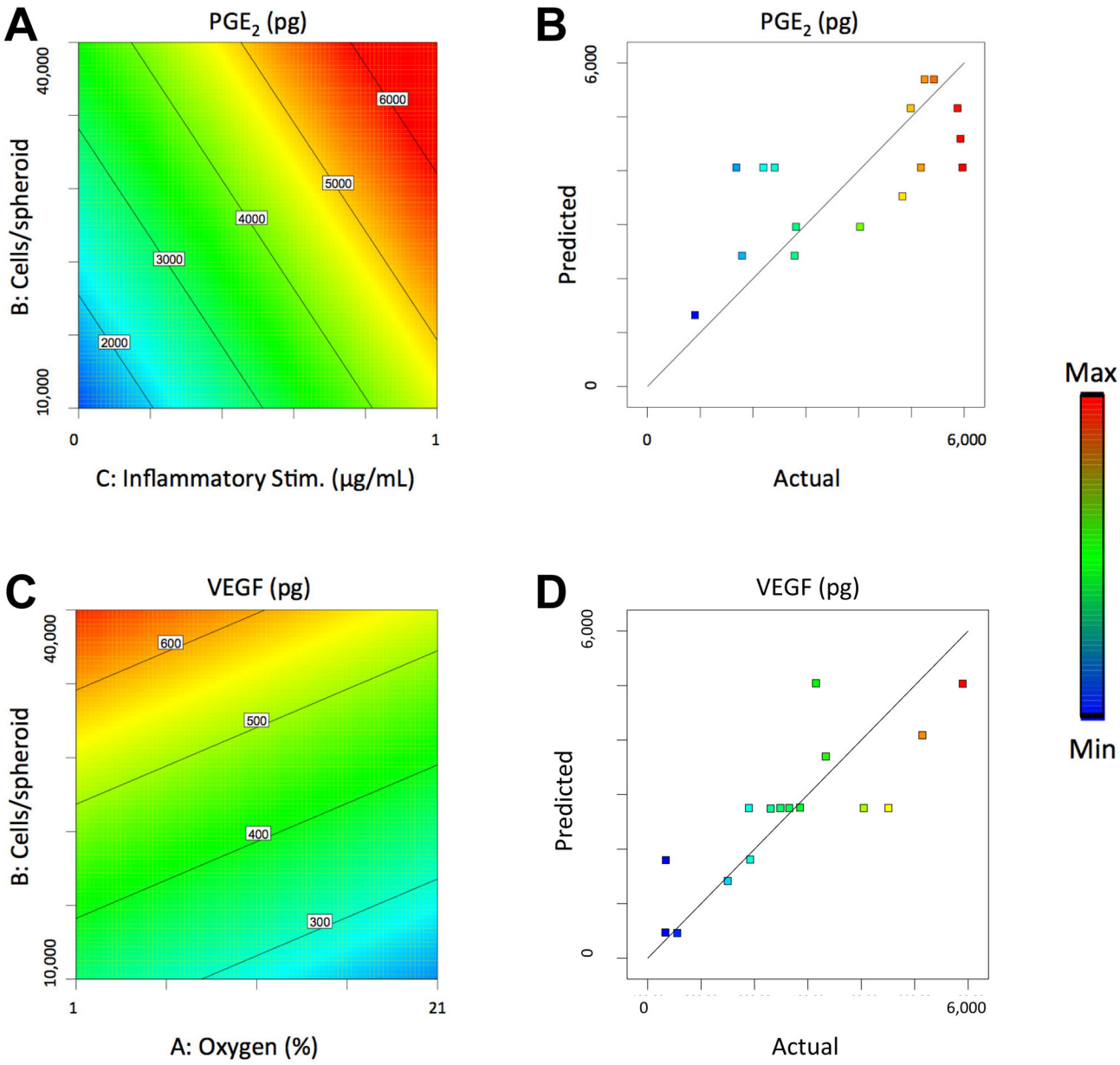

Figure 1. Response surface maps of microenvironment effects on the wound healing potential of MSC spheroids

(**A**) The effect of cells/spheroid and inflammatory stimulus on PGE_2 secretion by MSC spheroids. (**B**) PGE_2 Model Fit as visualized by plotting predicted versus actual PGE_2 values. (**C**) The effect of cells/spheroid and oxygen tension on VEGF secretion by MSC spheroids. (**D**) VEGF Model Fit as visualized by plotting predicted versus actual VEGF values.

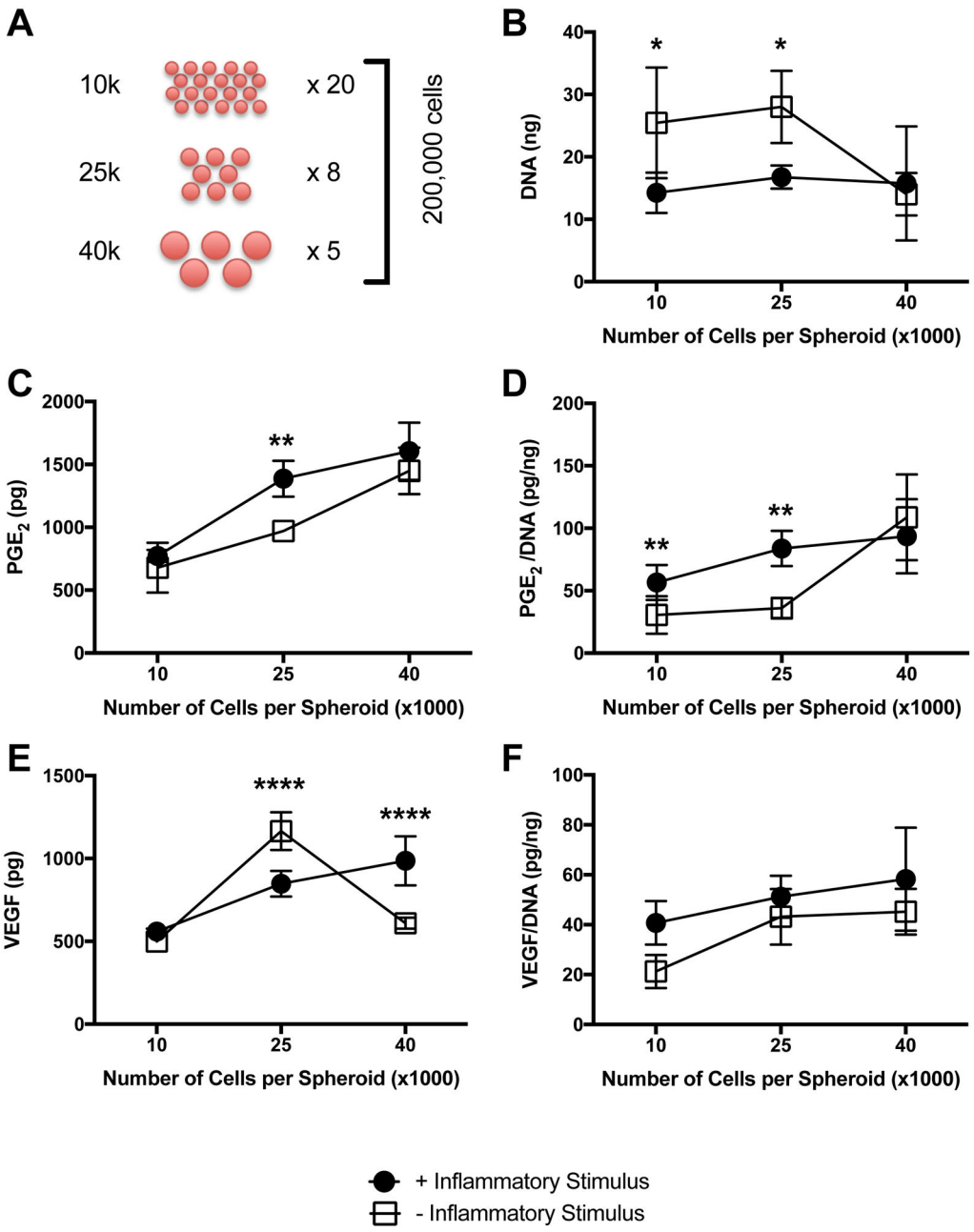

Figure 2. Secretion of proangiogenic and anti-inflammatory factors increases with spheroid size

(**A**) Diagram illustrating experimental approach to assess role of MSC number per spheroid on spheroid function. (**B**) DNA content as a function of spheroid size and inflammatory stimulus (*p<0.05 vs. +Inflammatory Stimulus for 10,000 and 25,000 cells per spheroid). Wound healing potential as quantified by (**C**) Total PGE_2 (**p<0.01 vs. +Inflammatory Stimulus for 25,000 cells per spheroid); and (**D**) normalized PGE_2 (**p<0.01 vs. +Inflammatory Stimulus for 10,000 and 25,000 cells per spheroid). (**E**) Total VEGF (****p<0.0001 vs. +Inflammatory Stimulus for 25,000 and 40,000 cells per spheroid). (**F**) Normalized VEGF. All data are n=4.

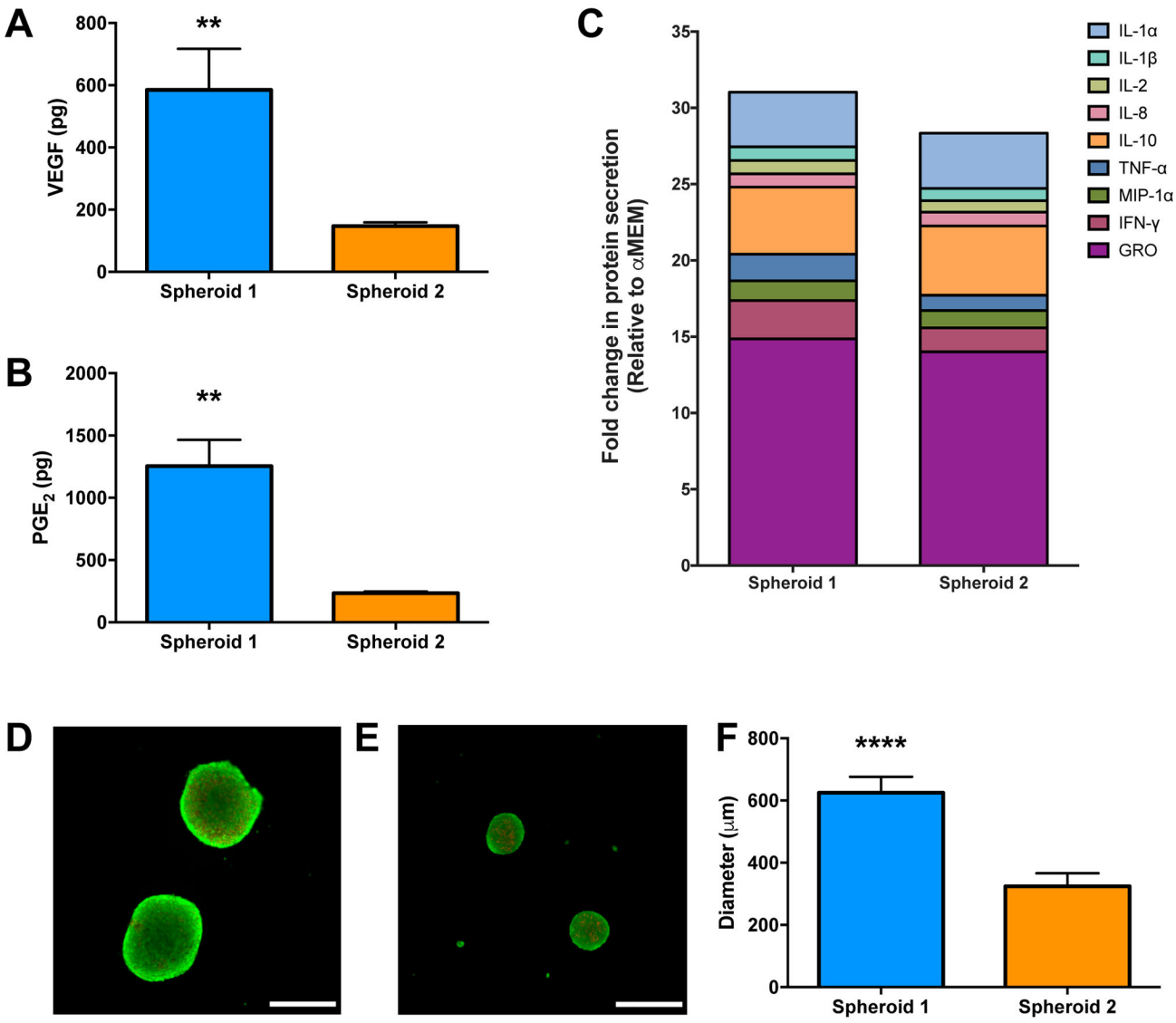

Figure 3. Validation of the DOE model using spheroids predicted to have the greatest (Spheroid 1) and least (Spheroid 2) VEGF and PGE_2 production

Spheroid 1 (40,000 MSCs/spheroid, 1 μg/mL Pam_3CSK_4, 1% O_2) versus Spheroid 2 (10,000 MSCs/spheroid, 0 μg/mL Pam_3CSK_4, 21% O_2). (**A**) VEGF and (**B**) PGE_2 were significantly increased in Spheroid 1 versus Spheroid 2 (n=4, ** $p<0.01$ vs. Spheroid 2). (**C**) Stacked column chart of predominant anti-inflammatory cytokines, normalized to unconditioned media (α-MEM). Live (*green*)/dead (*red*) assay showing the viability of (**D**) Spheroid 1 and (**E**) Spheroid 2. Scale bar represents 500 μm; images captured using a 4X objective. (**F**) Spheroid size is dependent upon the number of cells per spheroid (n=4, **** $p<0.0001$ vs. Spheroid 2).

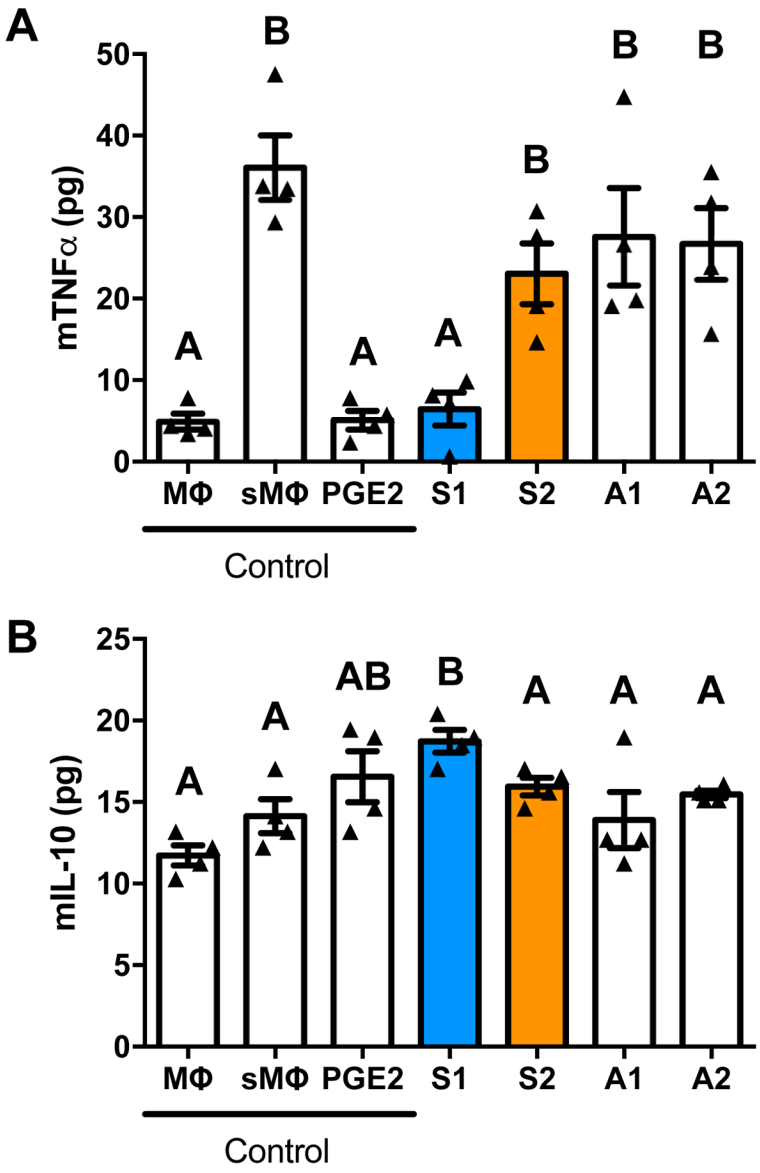

Figure 4. Macrophage phenotype is regulated by conditioned media (CM) from MSC spheroids

(**A**) Spheroid 1 CM reduced mTNFα secretion by LPS-stimulated murine macrophages, while CM from Spheroid 2 and adherent MSCs treated in the same manner were less effective. (**B**) Spheroid 1 CM stimulated secretion of IL-10 by LPS-stimulated macrophages significantly better than CM from Spheroid 2 and adherent MSCs treated in the same manner. Significance is denoted by alphabetical letterings; groups with no significance are linked by the same letters, while groups with significance do not share the same letters (n=4). Abbreviations: Mϕ, macrophage; sMϕ, stimulated macrophage; PGE_2, macrophages receiving 10 ng/mL PGE_2; S1, Spheroid 1; S2, Spheroid 2; A1, Adherent 1, cultured with 1 μg/mL Pam_3CSK_4, under 1% O_2; A2, Adherent 2, cultured with 0 μg/mL Pam_3CSK_4, under 21% O_2.

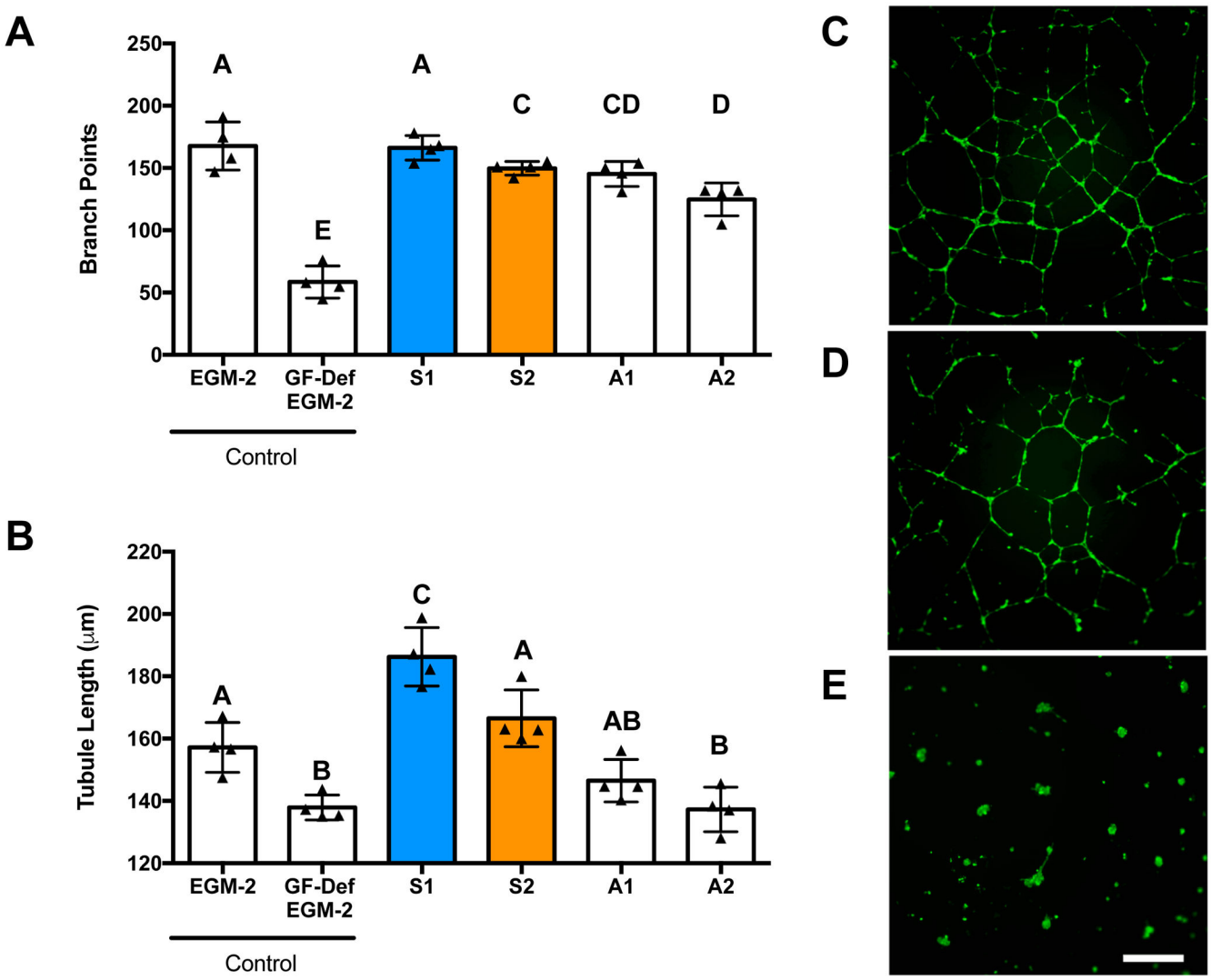

Figure 5. CM from optimized MSC spheroids promotes capillary network formation

Endothelial cell tubulogenesis in the presence of MSC-conditioned media measured by (**A**) the number of branch points per field of view and (**B**) total tubule length. Significance is denoted by alphabetical letterings; groups with no significance are linked by the same letters, while groups with significance do not share the same letters (n=4). Representative images of endothelial cell tubulogenesis on Matrigel in the presence of MSC-conditioned medium from (**C**) S1, (**D**) S2, and (**E**) EBM-2. Scale bar represents 500 μm; images captured using a 4X objective. Abbreviations: EGM-2, endothelial cell growth media, positive control; GF-Def EGM-2, growth factor deficient EGM-2, experimental control; EBM-2, endothelial basal media, negative control. S1, Spheroid 1; S2, Spheroid 2; A1, Adherent 1; A2, Adherent 2.

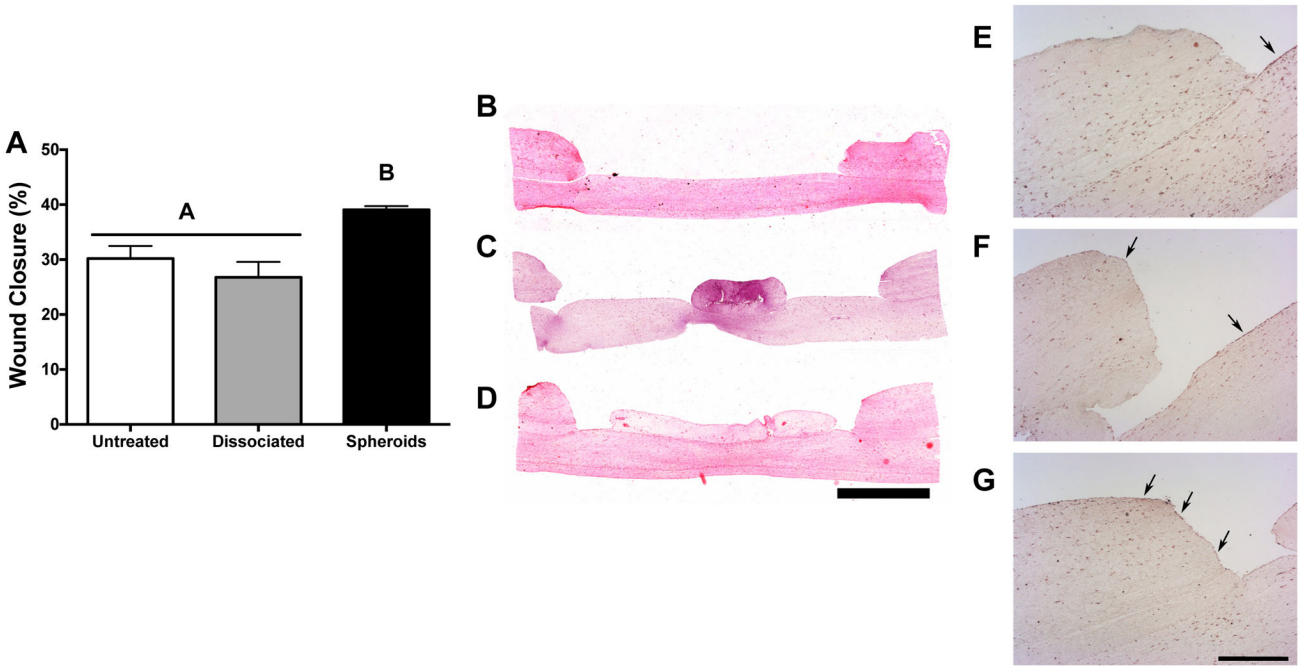

Figure 6. MSC spheroids promote healing and re-epithelialization in a human skin equivalent model

(**A**) Treatment of wounded HSEs with spheroid-loaded hydrogels increased wound closure after two weeks of co-culture. Representative H&E staining for HSEs that received (**B**) no treatment, (**C**) dissociated MSCs, or (**D**) MSC spheroids (Spheroid 1). Scale bar represents 2 mm; images captured using a 4X objective. Immunohistochemical staining of cytokeratin 10, denoted by black arrows, revealed re-epithelialization in defects that received (**E**) no treatment, **(F**) dissociated MSCs, or (**G**) MSC spheroids (Spheroid 1). Scale bar represents 500 μm; images captured using a 4X objective. Significance is denoted by alphabetical letterings; groups with no significance are linked by the same letters, while groups with significance do not share the same letters (n=4).

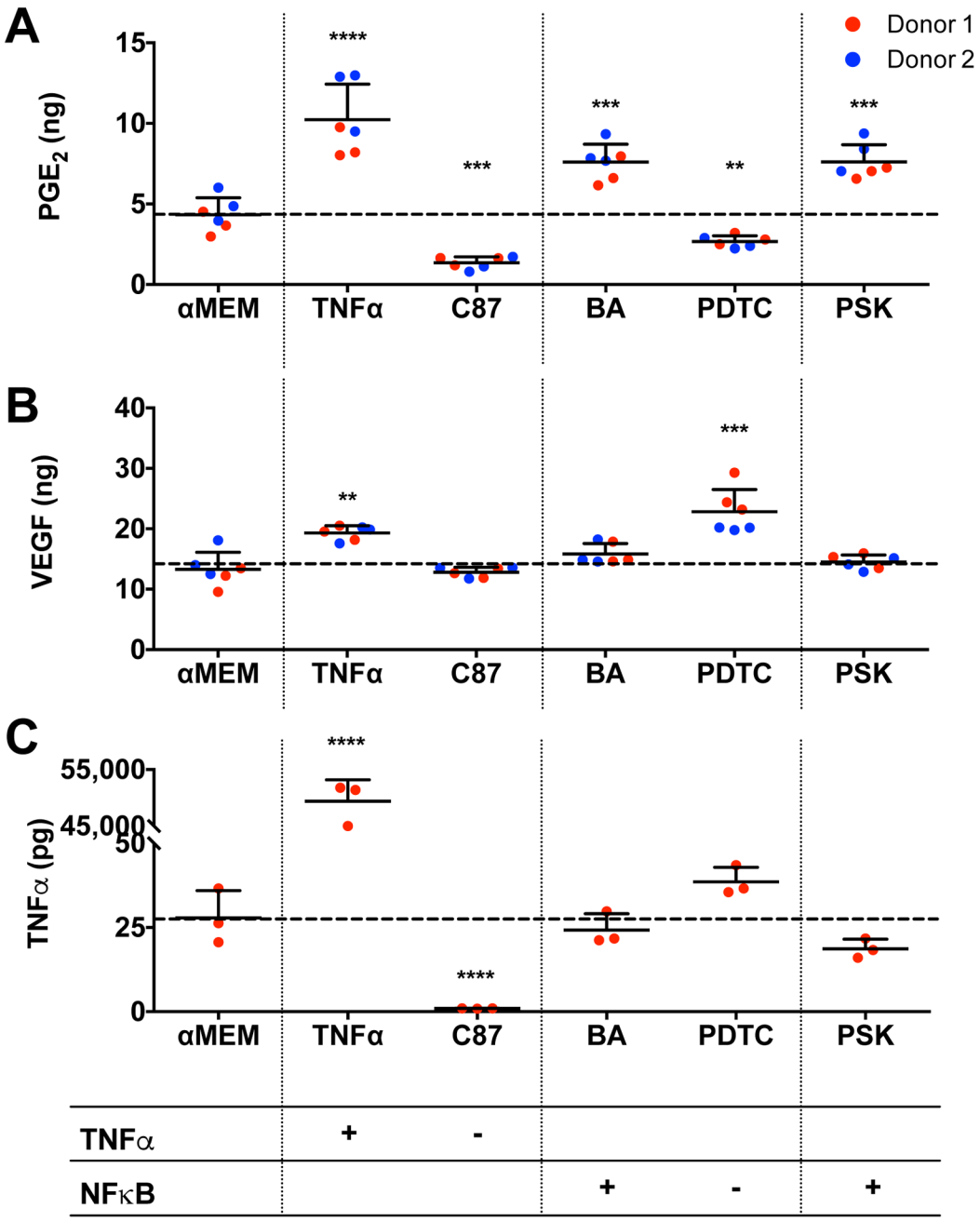

Figure 7. MSC spheroid secretion of PGE_2 is dependent on NFκB signaling

MSC spheroids containing 40,000 cells per spheroid and cultured in 1% oxygen (Spheroid 1) were treated with various agonists and antagonists of the NFκB and TNFα pathways. (A) Effect of stimuli on PGE_2 production (n=3 per biological donor; $^{**}p<0.01$ vs. α-MEM, $^{***}p<0.001$ vs. α-MEM, $^{****}p<0.0001$ vs. α-MEM). (B) Effect of stimuli on VEGF production (n=3 per biological donor; $^{**}p<0.01$ vs. α-MEM). (C) Effect of stimuli on TNFα production (n=3; $^{****}p<0.0001$ vs. α-MEM). Abbreviations: PSK, Pam_3CSK_4; BA, betulinic acid; PDTC, pyrrolidinedithiocarbamate.

Table 1

Stimulants/Inhibitors of TNFα and NFκB Pathways

Supplement	Pathway	Stimulant/Inhibitor	Concentration
TNFα	TNFα	Stimulant	50 ng/mL
C87	TNFα	Inhibitor	25 μM
BA	NFκB	Stimulant	100 μM
PDTC	NFκB	Inhibitor	1 mM
Pam_3CSK_4	NFκB	Stimulant	1 μg/mL